

Arnold flow

Authors: Markus Ernstsson, Weiyi Cui

FYST13
August 17, 2020



LUND
UNIVERSITY

1 Introduction

Chaos theory has many applications in different fields nowadays. For example, chaos plays an important role in the study of geology by e.g. describing the phenomenon of earthquakes in geology^[1] or biological population dynamics.^[2] In fact, chaos theory is widely practised in robotics as well. Different mathematical models have been tested in a controller to achieve chaotic behavior on robots. Such mobile robots with chaotic trajectories can be used as patrol robot or cleaning robots in a closed space.^[3] In this report, we focus on the application of the Arnold equation in a chaotic mobile robot designed by Y. Nakamura and A. Sekiguchi.^[3] The simulated trajectory of the chaotic robot is reproduced and compared to the trajectory presented by a random walker.

2 Theory

2.1 Motion of the robot

First, equation 1 is used to define the motion of the robot,

$$\begin{pmatrix} \dot{x} \\ \dot{y} \\ \dot{\theta} \end{pmatrix} = \begin{pmatrix} \cos \theta & 0 \\ \sin \theta & 0 \\ 0 & 1 \end{pmatrix} \begin{pmatrix} v \\ \omega \end{pmatrix} \quad (1)$$

where (x, y) is the position of the robot and θ is the angle between the velocity (v) of the robot and x . ω is the angular velocity of the robot.

2.2 Arnold–Beltrami–Childress (ABC) flow

Originally, the ABC flow is introduced as an exact solution to the three-dimensional Euler's equation of fluid particles. It actually leads to a chaotic Langrangian structure with a given Eulerian description, which means the positions of the fluid particles will become unpredictable after some period of time.^[4] The ABC flow is defined as,

$$\begin{pmatrix} \dot{x}_1 \\ \dot{x}_2 \\ \dot{x}_3 \end{pmatrix} = \begin{pmatrix} A \sin x_3 + C \cos x_2 \\ B \sin x_1 + A \cos x_3 \\ C \sin x_2 + B \cos x_1 \end{pmatrix} \quad (2)$$

where x_1, x_2, x_3 are the positions of the particle and A, B, C are constants. Typical trajectories of the ABC flow are shown in figure 1 and figure 2. According to Nakamura and Sekiguchi,^[3] when C is small, the ABC flow shows periodic motion and it shows chaotic motion when C is large. Our results confirm the phenomenon. We also use codes to present the Poincaré section with $x_2 = 0$, as figure 3 and figure 4 show.

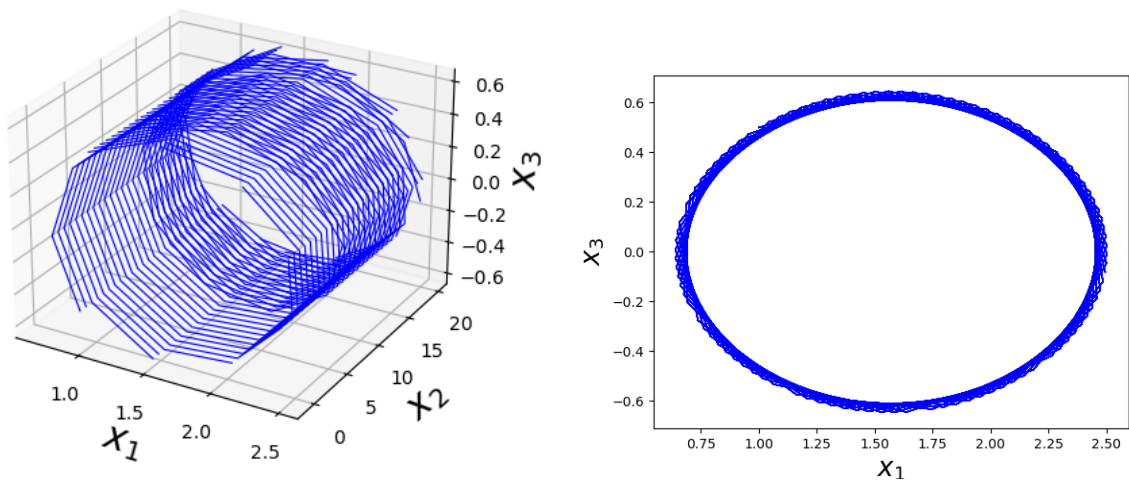


Figure 1: Trajectories of the ABC flow with $A=1$, $B=0.5$ and $C=0$.

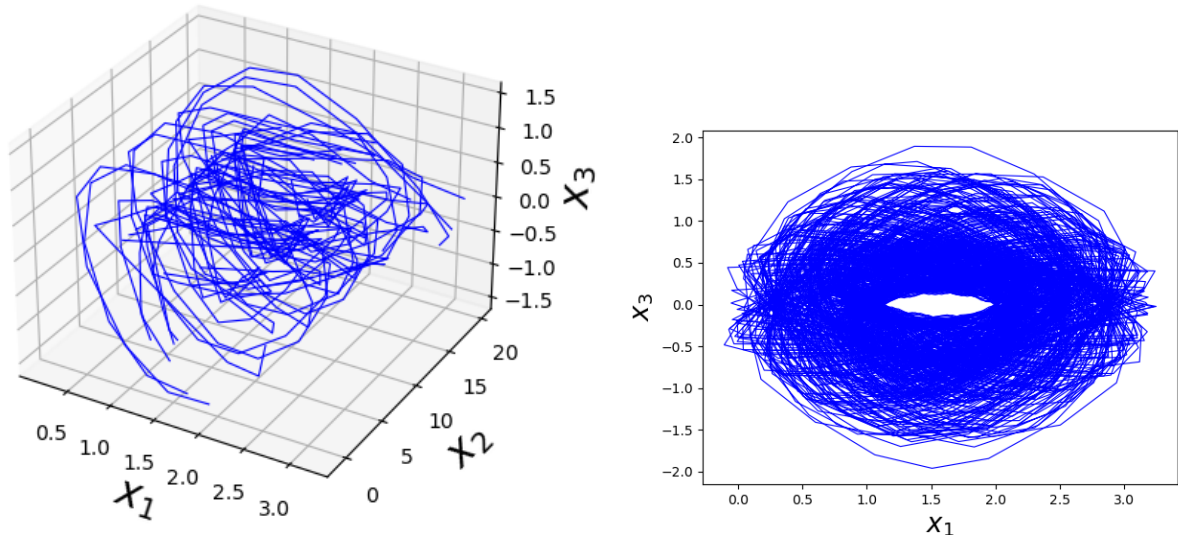


Figure 2: Trajectories of the ABC flow with $A=1$, $B=0.5$ and $C=0.5$.

As one can see, when $C = 0$, the trajectories in the Poincaré section are closed, but when C gets larger, there appears trajectories between the ellipses which are not closed. These scattered discrete points lead to the chaotic behavior.

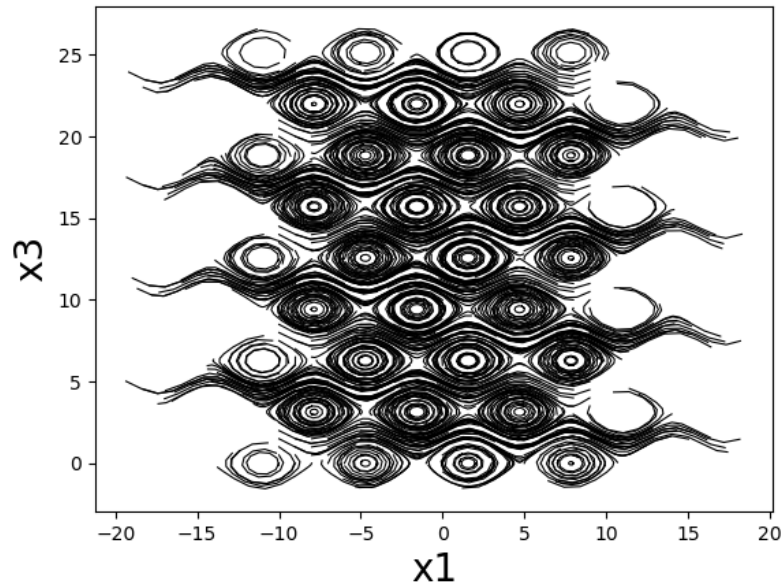


Figure 3: Poincaré section of the ABC flow with $A=1$, $B=0.5$ and $C=0$.

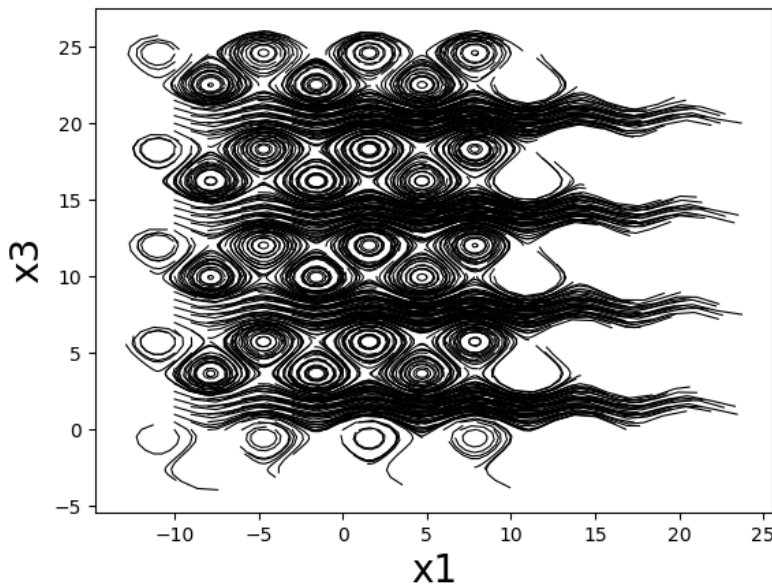


Figure 4: Poincaré section of the ABC flow with $A=1$, $B=0.5$ and $C=0.5$.

2.3 Stability analysis

Considering the Poincaré sections in figure 3 and 4, one can write the system into

$$\begin{pmatrix} \dot{x}_1 \\ \dot{x}_3 \end{pmatrix} = \begin{pmatrix} A \sin x_3 + C \\ B \cos x_1 \end{pmatrix}. \quad (3)$$

Thus, the Jacobian is

$$\mathbf{Df}(x) = \begin{pmatrix} 0 & A \cos x_3 \\ -B \sin x_1 & 0 \end{pmatrix}, \quad (4)$$

and the eigenvalues are $h = \pm\sqrt{-AB \sin x_1 \cos x_3}$. This indicates that the system with $x_2 = 0$ is conserved since the sum of h is zero. This shows again the discrete trajectories in the chaotic region in figure 4 will not be attracted.

Furthermore, the Lyapunov exponent of the ABC flow (equation 2) can be calculated according to equation (4.54) in the textbook *Chaos*.^[5] Figure 5 shows the numerical approach to the largest Lyapunov exponent based on J. C. Sprott's program.^[6] The result converges to 0.00532 after 5000 iterations. The positive λ leads to the sensitive dependence on initial conditions for the ABC flow.

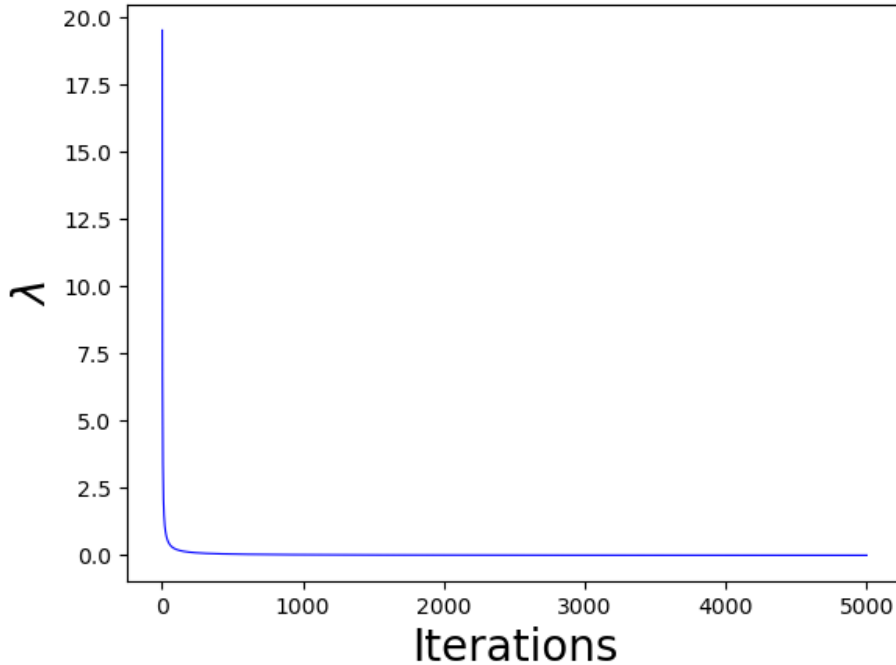


Figure 5: The largest Lyapunov exponent λ for the ABC flow after 5000 iterations with a time step of 1. $A = 0.5, B = 0.25$ and $C = 0.25$. The initial condition is $x_1 = 4, x_2 = 3.5, x_3 = 0$. λ converges to 0.00532.

3 Method

The ABC flow is integrated into the motion of the robot as

$$\begin{pmatrix} \dot{x}_1 \\ \dot{x}_2 \\ \dot{x}_3 \\ \dot{x} \\ \dot{y} \end{pmatrix} = \begin{pmatrix} A \sin x_3 + C \cos x_2 \\ B \sin x_1 + A \cos x_3 \\ C \sin x_2 + B \cos x_1 \\ v \cos x_3 \\ v \sin x_3 \end{pmatrix}. \quad (5)$$

The chaotic trajectory is numerically solved and compared to the one generated by a random walker. A random walker drives the motion of the robot with a random selection of the direction of the motion. Both the chaotic and the random trajectories evolve unrestrictedly, and afterwards a mirror mapping is applied, which means the trajectory is mirrored at the boundary of the confined space. Intercepts at the boundary are also generated by fitting the two positions before and after linearly. Different obstacles are also introduced to simulate the robot's motion in a more realistic environment.

In order to compare chaotic motion to random motion, we employed a scanning test. The test consists of having the chaotic and random robot move throughout an environment and check how efficiently they scan the available area. This scanning test is performed for various courses and for different starting positions. The test is, however, carried out a bit differently for the random robot and the chaotic robot. For the random robot, a jackknife^[7] mean scan of several random walks is used in order to achieve an unbiased result. The chaotic trajectory is, though, numerically solved only once for each starting condition.

The whole numerical solution is conducted in Python.^[8]

4 Results & Discussion

The two robots scan four different environments from two different starting positions, in order to see if there is any difference depending on the course or the starting position. All courses are 25 by 25 unit length squares with differing amounts of obstacles: none, one central obstacle, two symmetrically placed obstacles, and three symmetrically placed obstacles. The different courses are shown in figure 6 with a chaotic trajectory and a random trajectory. The two starting positions are placed symmetrically about the central y -position of the environment ($y = 12.5$) in the y -direction: (5, 5) and (5, 20). For all the different environments, A , B , and C were constant as well as the starting values of x_1 , x_2 , and x_3 , as can be seen in table 1. These values are chosen so that the resulting trajectory in x_1 , x_2 , x_3 -space is chaotic. It was also confirmed that the trajectory in xy -space behaved chaotically by making sure that it covered the whole space, no matter the obstacles or the starting position in xy -space.

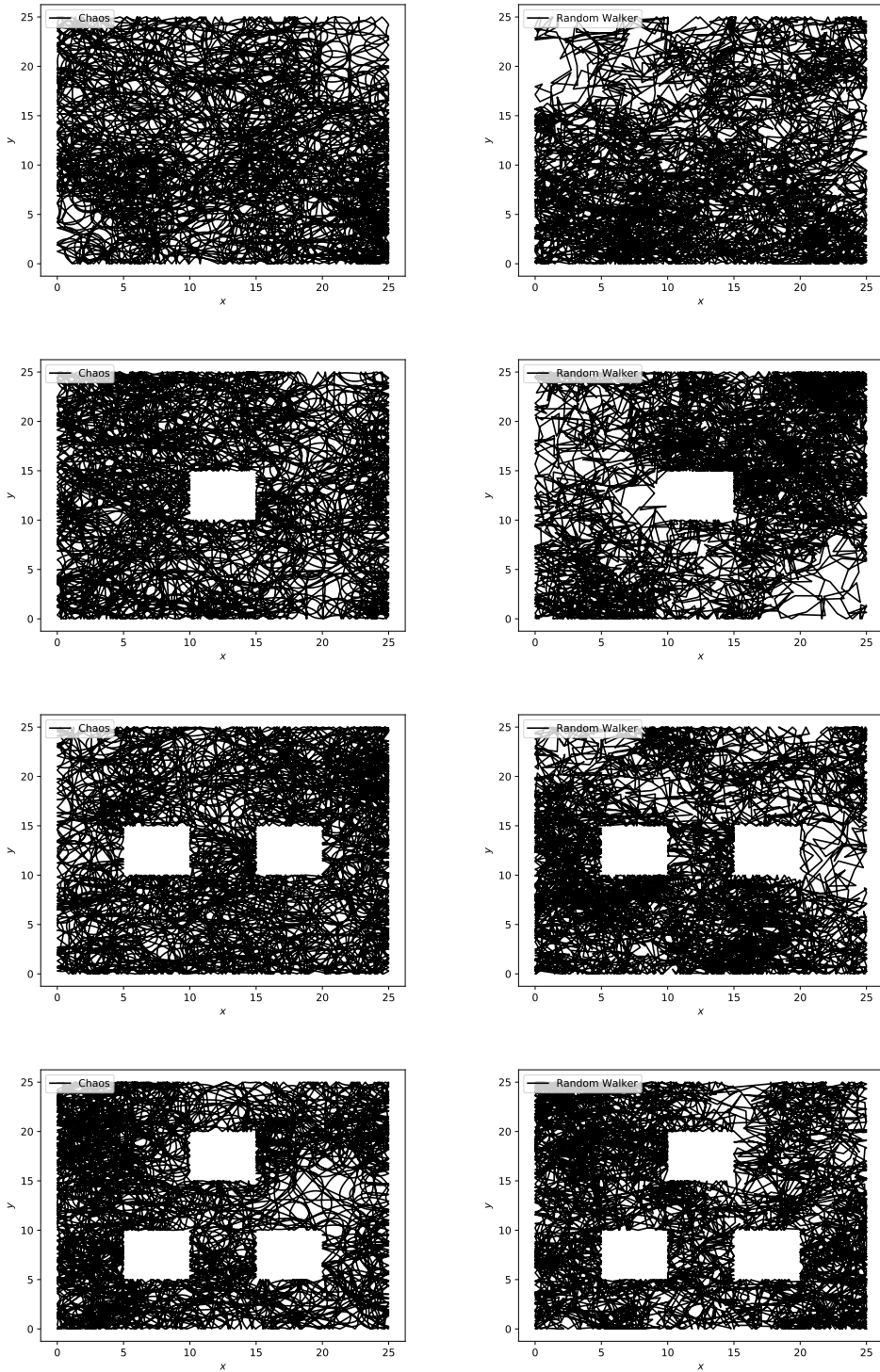


Figure 6: Trajectories of the chaotic robot (left) and the random robot (right) for the four different courses. The chaotic trajectories appear to cover the available areas more uniformly.

Table 1: Constant values used in the scanning tests. The x 's and the y are starting values for the variables. The left-hand side shows the constants for the chaotic robot, while the right-hand side shows the constants common for both robots.

A	B	C	x_1	x_2	x_3	x	y	v
1	0.5	0.5	4	3.5	0	5	5, 20	1

In figure 7, the scanning efficiency of the two robots for the different environments from the different starting positions are shown. In general, the random robot is less efficient than the chaotic robot, however, the chaotic robot is more sensitive of the starting position. Note that the largest deviation between the two starting positions for the chaotic robot is in the environment with three obstacles. This is due to the other environments being invariant to the starting position, as can be seen in figure 6. There appears to be little to no difference for the random robot in the different courses. Figure 8 displays the scanning efficiency of the random robot for the two different starting positions in the environment with no obstacles and the one with three. Indeed, there is a very slight difference between all of the scans, but nothing significant.

As far as the chaotic trajectories are concerned, in figure 9 the scanning efficiencies of the chaotic robot in the different environments are plotted. As is shown, there is no large difference for the environments with the smaller amounts of obstacles; however, there is a dramatic shift in efficiency for the three obstacles environment compared to the other environment.

5 Conclusion

Based on our results, we can conclude that a chaotic robot is usually more efficient at scanning an area than a random robot. However, a chaotic robot is far more sensitive to the starting position than a random robot. Yet, a chaotic trajectory is deterministic, and as such, it will always perform the same (given that the initial conditions are the same). Compare this to a random trajectory which will differ each run and is therefore not reliant.

In short, a robot controlled by a chaotic ABC flow has the possibility to be superior than one controlled by a random walker. The conclusion agrees to Y. Nakamura and A. Sekiguchi's work.^[3]

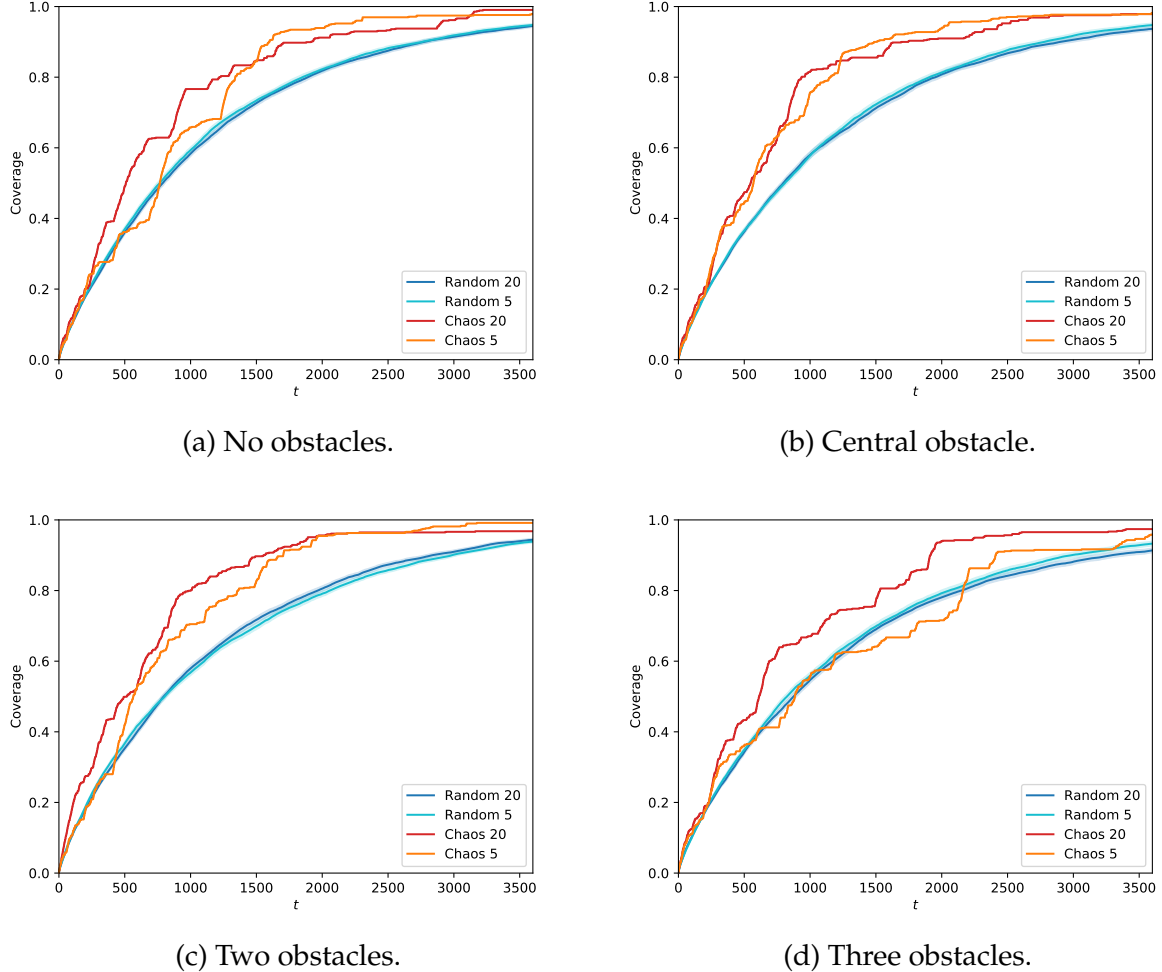


Figure 7: The amount of the total available area covered as a function of time for the four different environments. The shaded bands of the random curves are the statistical uncertainties of the jackknife mean. As the chaotic trajectory is deterministic, there is only a single run, hence the rough curves. There is no perceivable difference in regards to the starting point for the random robot.)

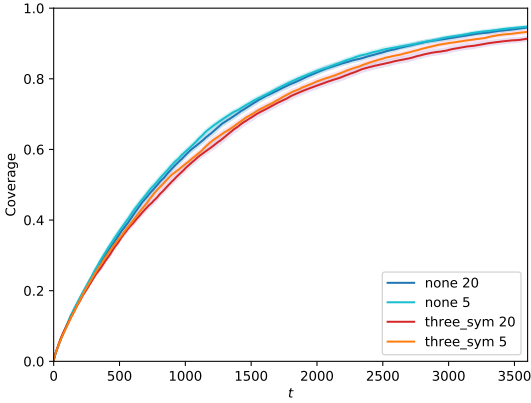


Figure 8: The amount of the total available area covered by a random robot as a function of time for the no obstacle and the three obstacles environments. There is no major difference in the efficiency for the two environments, indicating that a random robot scans equally well regardless of the environment.

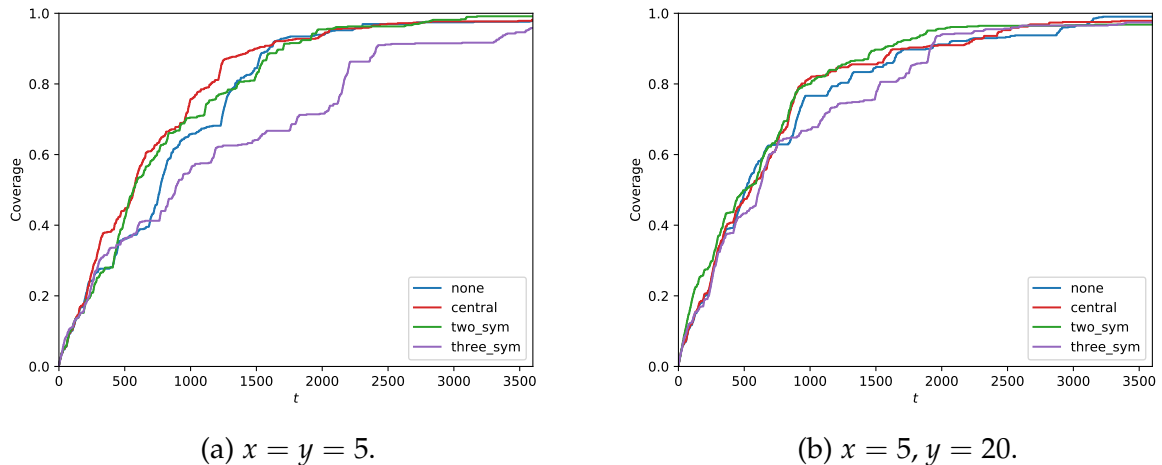


Figure 9: The amount of the total available area covered by a chaotic robot as a function of time for the four different environments separated by the starting position. There is no major difference in the scanning efficiency of the no obstacle, central obstacle, and the two symmetric obstacles environments. However, there is a clear loss in efficiency for the three obstacles environment.

References

- [1] D. L. Turcotte, *Fractals and Chaos in Geology and Geophysics*, 2nd ed. Cambridge University Press, 1997.
- [2] R. M. May, "Chaos and the dynamics of biological populations," *Nuclear Physics B - Proceedings Supplements*, vol. 2, pp. 225 – 245, 1987. [Online]. Available: <http://www.sciencedirect.com/science/article/pii/092056328790020X>
- [3] Y. Nakamura and A. Sekiguchi, "The chaotic mobile robot," *IEEE Transactions on Robotics and Automation*, vol. 17, no. 6, pp. 898–904, Dec 2001.
- [4] X.-H. Zhao, K.-H. Kwek, J.-B. Li, and K.-L. Huang, "Chaotic and resonant streamlines in the abc flow," *SIAM Journal on Applied Mathematics*, vol. 53, no. 1, pp. 71–77, 1993. [Online]. Available: <http://www.jstor.org/stable/2102274>
- [5] G. Ohlén, S. Åberg, and P. Östborn, *Chaos*. Lund university, 2007.
- [6] "Lyapunov exponent and dimension of the lorenz attractor," <http://sprott.physics.wisc.edu/chaos/lorenzle.htm>, accessed: 2005-05-27.
- [7] R. G. Miller, "A trustworthy jackknife," *Ann. Math. Statist.*, vol. 35, no. 4, pp. 1594–1605, 12 1964. [Online]. Available: <https://doi.org/10.1214/aoms/1177700384>
- [8] G. Van Rossum and F. L. Drake, *Python 3 Reference Manual*. Scotts Valley, CA: CreateSpace, 2009.